Manipulating carbon nanotubes Towards the application as novel field emission sources

Heeres, E.C.

1

Introduction

In an electron microscope (EM), samples and processes are imaged or studied with a resolution of several nanometers, or even a fraction of a nanometer, depending on the type of microscope and sample.[1] Besides imaging, other applications exist, such as the analysis of materials and processes, device testing, sample fabrication, deposition, and etching.

In this chapter some basic EM-principles and applications will be discussed first, after which the electron sources are treated in *Section 1.2*. Starting with the state-of-the-art sources, we will address the need for novel electron sources and introduce the (novel) materials in *Section 1.3 and 1.4,* which have been used throughout the research that is presented here. In *Sections 1.4 and 1.5* our research questions are posed, followed by a brief summary of the results and an overview of the project of which this research was a part in *Section 1.6*. Finally, in *Section 1.7*, the contents of the following chapters in this thesis are described.

1.1 Electron beams and applications

The key advantage of an electron microscope over a light microscope is the use of a beam of electrons, which behave like waves with much shorter wavelengths than photons in visible light. Using the equation for a free electron gas, the (relativistic) electron wavelength can be written as:[2]

$$\lambda = \frac{h}{p} = \frac{hc}{pc} = \frac{hc}{\left(E_{\text{kin}}{}^2 + 2E_{\text{kin}}m_0c^2\right)^{1/2}} \tag{1.1}$$

where λ is wavelength, h Planck's constant, c the speed of light in vacuum, E_{kin} the kinetic energy, and m_0 the electron rest mass. An electron with a kinetic energy of 200 keV has a corresponding wavelength of 2.5 pm, which is five orders of magnitude lower than the wavelength of a photon in visible light ~ 10^2 nm. Because of this difference in wavelength, the diffraction limit – being the fundamental resolution limit of an optical system that scales linearly with wavelength – is lower for electrons, and hence a higher resolution can be obtained using electron microscopy. However, this fundamental limit is not reached due to aberrations by imperfections in electron lenses which standard electron microscopes do not correct for. Chromatic and spherical aberrations cause the achievable resolution limit in a non-corrected electron microscope to be about 100 times higher than the electron wavelength.[3] Note that recent developments have led to systems for the correction of chromatic- and spherical aberrations.[4]

Three basic types of electron microscopes exist:

- Transmission electron microscope (TEM)
- Scanning electron microscope (SEM)
- Scanning transmission electron microscope (STEM)

In a TEM, displayed schematically in Figure 1.1a, the electron beam is transmitted through a section of the sample, hence restricting its thickness to approximately 100 nanometers, followed by a magnification and projection onto a phosphor screen or CCD camera. Both above the sample – for probe forming – and underneath – for

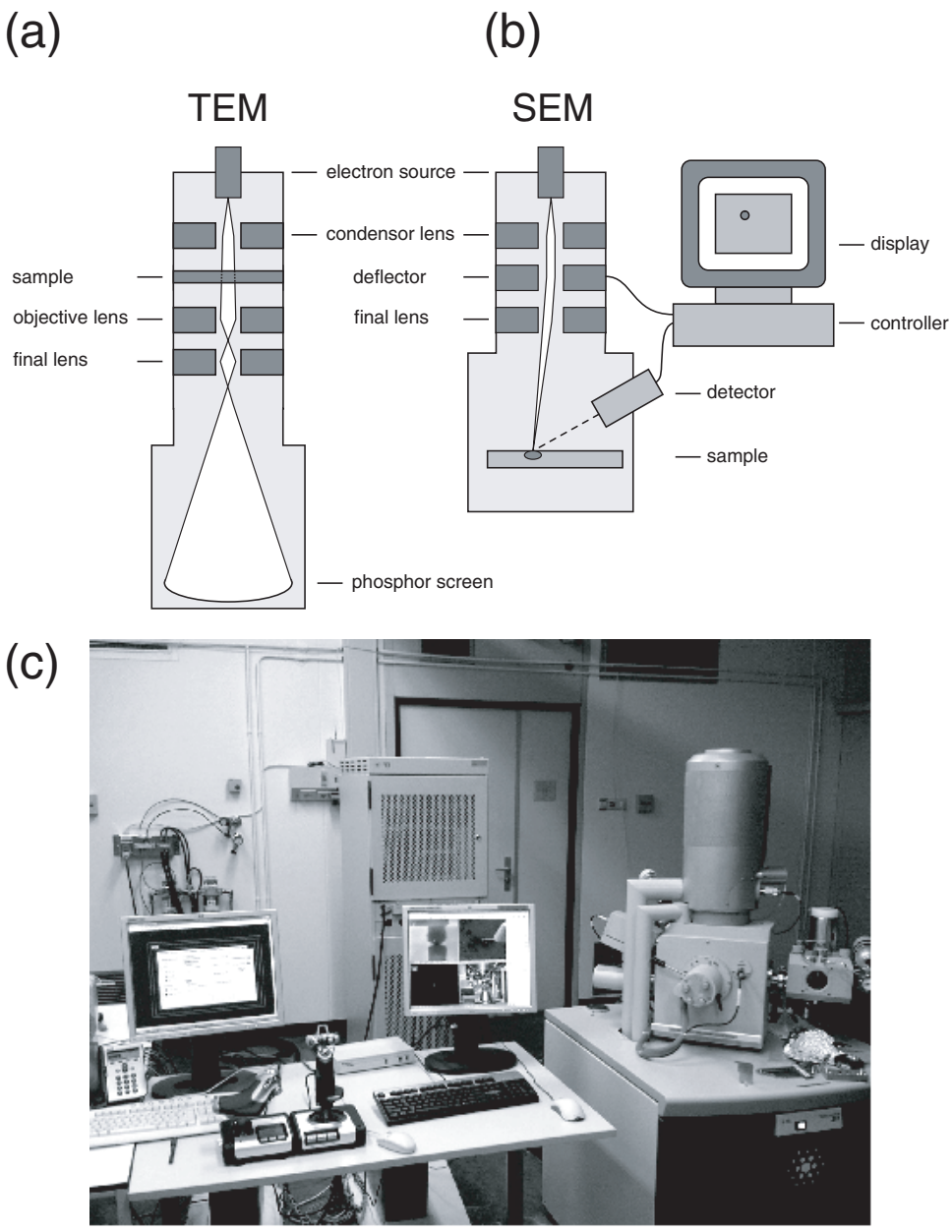

Figure 1.1 (a),(b) Schematic representation of a transmission electron microscope (TEM) and a scanning electron microscope (SEM). (c) Photograph of the SEM at Leiden University. The joysticks in between the two keyboards are used to operate the nanomanipulator inside the SEM.

projection – lenses are placed within short distances, hence enabling small focal lengths and keeping aberrations low, but restricting the overall size and movement of sample and holder within the millimeter range. The SEM employs a system to focus the electron beam into a spot with a typical diameter of about 1 nm (probe) and to deflect it in such a way as to scan the sample point by point and line by line, as shown schematically in Figure 1.1b. At each point of this scan, the electron signal collected at a detector – installed inside the vacuum chamber – is a measure for the intensity of the image that is generated point by point. Due to the layout of the SEM, usually with one lens column several millimeters to centimeters above the sample, the use of larger samples and larger movements are allowed. Compared with TEM, an SEM uses lower beam energies, typically ranging from 1 keV up to 30 keV, with corresponding lower resolution as a result. The resolution capabilities of both instruments are sketched in Figure 1.2.[5-7] Shown in Figure 1.1c is the setup of our SEM in Leiden. The scanning transmission electron microscope (STEM) uses an electron probe to scan the sample, as in an SEM, and subsequent recording of the transmitted electron beam. Recently, an experiment showing a resolution below 50 pm was published, using a TEM at 300 keV in scanning probe mode (STEM), corrected for spherical and chromatic aberrations.[8]

Apart from obtaining structural information of a sample, electron microscopes are often used for chemical analysis techniques,[9] based on interactions of the electron beam with the atoms in the specimen, such as electron energy loss spectroscopy (EELS), and energy dispersive x-ray spectroscopy (EDX). In EELS, the energy spectrum of the reflected/transmitted electron beam is studied for electron energy loss due to inelastic interactions with the species of the sample, like phonon excitations and ionization of inner shell electrons.[10] In EDX, the spectrum of x-ray radiation originating from electron interactions with the species of the sample is analyzed.

Also, electron beams focused into nanometer spots can be used for electron beam lithography. In such a system, the electron beam is used to define a pattern on a sample with an electron-sensitive resist by moving both the electron beam (deflection) and the stage (translation) with respect to each other. In this way,

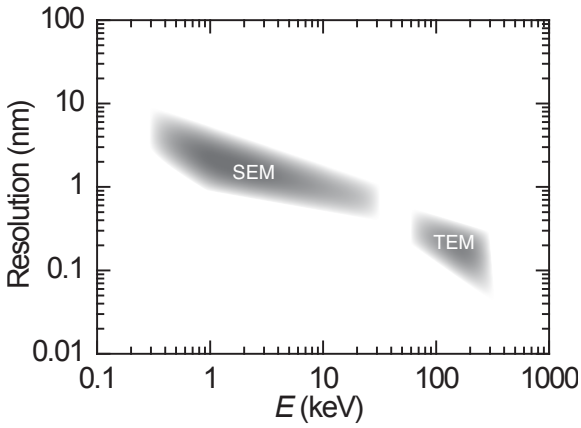

Figure 1.2 Indication of SEM and TEM resolution ranges as a function of electron beam energy.

structures with dimensions of 10 nm and smaller can be defined without the use of a mask.[11,12]

Finally, one of the first setups to study surfaces with near-atomic resolution was the field emission microscope (FEM),[13] which was also used throughout the research presented in this thesis to study the relation between an electron source and the electron beam emitted from it. To achieve this, a sharp tip (source) is placed in a high electric field inside a vacuum chamber, causing field emission of electrons; this electron beam is then imaged using a phosphor screen.

1.1.1 Electron beam-specimen interactions

Due to the interaction of an incident electron beam with the atoms in a specimen, a wide range of signals is available for imaging and analysis, see Figure 1.3. Some incident electrons are reflected or scattered back elastically – without loosing energy – also known as backscattered electrons (BSE). Other incident electrons loose energy by inelastic scattering events, knocking out electrons from the atoms of the specimen; the latter being secondary electrons (SE) and Auger electrons. Besides elastic and inelastic reflection of electrons, also transmission of both types exist which can be used in different ways for image formation.[14] Characteristic x-rays, generated within the interaction volume, can be used to map the elemental

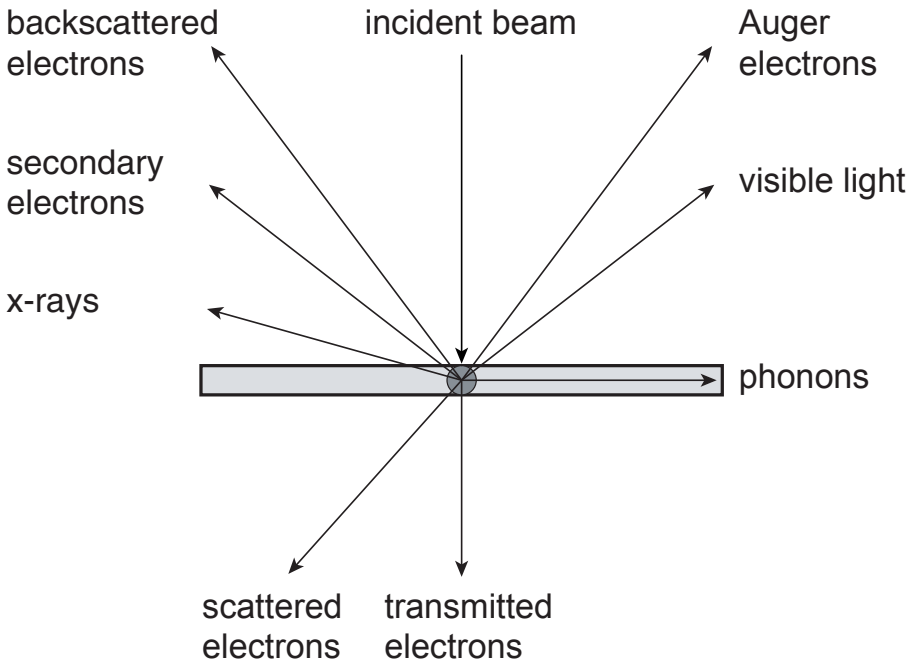

Figure 1.3 Schematic representation of the interactions of an incident electron beam with a specimen.

distribution of the sample with an EDX detector. If the sample is thin enough, electrons can be transmitted through the sample which is a prerequisite for the transmission electron microscope, as the transmitted electrons are used for imaging. Also for the scanning electron microscope, transmission detectors are available to perform scanning transmission electron microscopy (STEM), offering sub-nanometer resolution at ~30 keV beam energies, while restricting sample sizes.[15]

In Chapter 5, experiments are described in which the electron beam has been used to cut through carbon nanotubes.

1.2 Electron sources

In this section, the different types of electron emission will be discussed, as well as the key requirements for electron sources. Hereafter, the common commercially

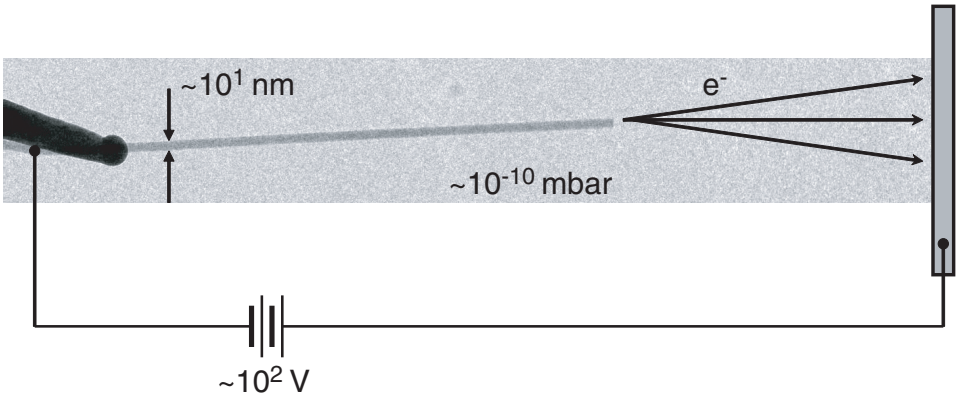

Figure 1.4 Schematic representation of an electron field emitter. Mounted onto a sharp tip is a high aspect ratio nano-object, i.e. a nanotube or -wire, with a typical diameter of several nanometers. In a vacuum chamber at a pressure of 10^{-10} mbar, electrons are emitted towards the anode, typically by applying an extraction voltage of several hundred volts.

used sources are compared.

1.2.1 Electron emission and source types

In an electron source, electrons are extracted from a solid material (cathode) and accelerated into vacuum towards an anode, creating an electron beam. In Figure 1.4 a nanowire emitter is shown, drawn within a schematic extractor setup. Several extraction mechanisms exist, that differ in the way which electrons pass the potential barrier between the cathode surface and vacuum. One way is to give the electrons sufficient energy to overcome the potential barrier; another way is to modify the potential barrier in such a way as to enable electron tunneling. The potential difference between the Fermi energy E_F and the vacuum is called the work function ϕ. In the first case, the electron energy is elevated by a high temperature or photon irradiation; called thermionic emission and photoemission, respectively. In the second case, the potential barrier is modified by an electric field. The electrons in the source placed within the attractive electric field will still see a barrier, but its width is reduced depending on the electric field strength, see Figure 1.5. Lower energy electrons will see a wider potential well, whereas higher energy electrons will see a thinner potential well, and have a higher tunneling probability.[16]

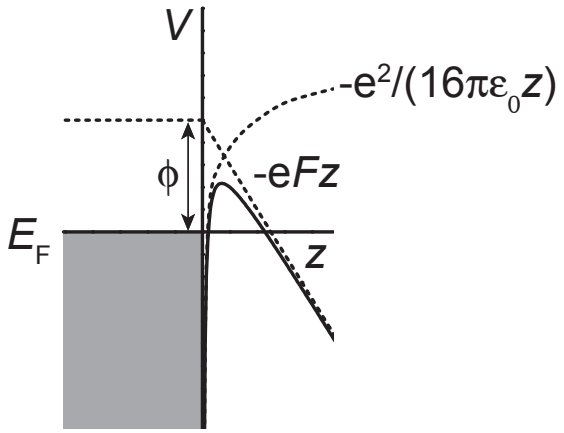

Figure 1.5 Potential for an electron outside the emitter as a function of distance from the emitter surface. The potential is made up of two parts: the image charge potential and the potential due to the applied electric field. Also indicated are the Fermi energy E_F and the workfunction ϕ. For simplicity the Fermi-Dirac distribution at 0 K is drawn and the filled (metallic) states are indicated in grey.

Electrons around the Fermi energy will be emitted, where the temperature (Fermi-Dirac distribution drawn for $T = 0$ K) determines the high-energy part of the field emission energy spectrum and the tunneling parameter[17] determines the low-energy part of the spectrum. This type of emission is called (cold) field emission. Schottky- or thermal field emission is the combination of emission at an electric field and at a high temperature.[18]

To improve upon the capabilities of electron microscopes, we first need to address the key requirements for a good electron source. These are: high brightness, low energy spread, high stability, and a long lifetime. Higher brightness will lead to more current in the same spot, and as a result faster imaging, analysis, or e-beam writing is possible. A low energy spread reduces chromatic aberrations. Stability can be divided in short- and long-term stability. Short-term stability is needed for proper measurements, as instabilities cause measurement errors. Long-term stability determines the time a source can be operated and hence affects its lifetime. With a longer lifetime, the source needs to be replaced less often and because of this it is more user-friendly and cheaper.

Table 1.1 List of characteristic parameter values for three most used commercial electron sources; the Schottky emitter, cold field emission gun (CFEG), and the LaB_6 emitter. Source: N. de Jonge.[19]

	Schottky	CFEG	LaB_6
Energy spread (eV)	0.4 – 0.7	0.25 – 0.3	1.0
Reduced brightness ($A \cdot m^{-2} \cdot Sr^{-1} \cdot V^{-1}$)	$(0.3 – 1.0) \times 10^8$	$(1 – 2) \times 10^8$	10^5
Geometric source size radius (nm)	900	50	15000
Virtual source size radius (nm)	15	2.5	10^4
Emission stability short term (%RMS)	< 1	3 – 5	< 1
Typical lifetime (h)	> 5000	> 1000	200
Operating temperature (K)	~ 1800	~ 300	~ 1700
Operating vacuum level (mbar)	$< 10^{-8}$	$< 10^{-10}$	$< 10^{-6}$

Common commercially used emitters are the LaB_6 source, the tungsten (W) cold field emission gun (W-CFEG) and the Schottky emitter. These three sources are listed in Table 1.1 together with their parameters.[19] The first type uses a low workfunction crystal – lanthanum hexaboride – and usually has a large virtual source size and low brightness. The W-CFEG has a tip with a radius of curvature ~50 nm, where electrons are extracted within a strong electric field at low temperatures, i.e. cold FE. A low energy spread and high brightness are characteristic features of this source which is used in ultrahigh resolution instruments. Instabilities of the tip shape and emission surface require periodical reprocessing of the tip, hence this

source is not the most user-friendly one. The Schottky emitter has high brightness, but a higher energy spread than the W-CFEG. A tungsten tip, coated with a workfunction-lowering layer of ZrO and its radius $r \sim 0.5$ μm, forms the base of this source which is being used in many modern electron microscopes.[20]

1.2.2 Characterization of sources

To characterize an electron source, the parameters mentioned in the above have to be determined and compared. After fabrication of the source, it is transferred into a field emission test setup and cleaned from adsorbed species by heating. The presence of such species is indicated by changes in the emitted current and in the image of the field emission microscope, as adsorption and desorption events locally change the field emission properties of the tip. In dedicated FE-test setups current-voltage (I-V) characteristics are measured, together with angular current density, virtual source size, energy spread, current stability, and lifetime. Models for the field emission energy distribution (FEED) and FE current can be fitted to the data and used to obtain characteristics of the source, such as electric field strength, operating temperature, tunneling parameter, etc.. The stability of the source structure affects its lifetime and emission current stability. To obtain information about the source's structural stability during field emission, TEM images before and after field emission experiments can be compared, or the source can be tested in-situ, i.e. performing TEM imaging during electron emission.[21] Such structural information can be used to explain observations during field emission measurements and gives insight in the long-term stability of the source. This is why Feynman's quote "Just look at the thing" was used as an introduction to this thesis.

1.3 Carbon nanotubes

Carbon nanotubes[22-25] have unique mechanical and electronic properties, see the quantities listed in Table 1.2.[26-29] Due to their size and structure, these mechanical and electronic properties are of great interest for potential applications, one of which is their use as next-generation field emission sources.[30] A carbon nanotube can be considered as one single layer of graphite (graphene) rolled-up into a single cylinder, creating a single-walled carbon nanotube (SWNT). A multi-walled carbon

Table 1.2 Carbon nanotube parameters

	SWNT	MWNT
Minimum diameter (nm)	< 1	~ 2
Maximum current density[26,27] ($A \cdot cm^{-2}$)	> 10^9	10^9 - 10^{10}
Young's modulus[28] (Pa)	~ 10^{12}	~ 10^{12}
Tensile strength[28] (Pa)	~ 10^{10}	~ 10^{10}
Wall separation distance[29] (nm)	-	0.34

nanotube (MWNT) can be considered to consist of multiple SWNTs wrapped around each other to form concentric tubes. The shell or wall separation distance between adjacent tubes is roughly equal to the plane spacing of graphite, 0.34 nm. Both SWNTs and MWNTs are made out of covalently bound carbon atoms, in a two-dimensional hexagonal lattice with sp^2 type carbon-carbon bindings,[31] making them very stiff, chemically stable structures and able to carry large current densities up to 10^9 A/cm^2.[26,32] Most of all, they are known for their exceptionally high Young's modulus, up to 1 TPa for single CNTs.[28] When CNTs are combined into macroscopic bundles, the reported Young's modulus is significantly lower, around 80 Gpa. However, electron beam treatments have shown to be able to reinforce such bundles.[33,34] To close a rolled-up graphene sheet, i.e. to create closed caps, half a fullerene molecule is needed on each of its ends – one of which is C_{60}, Buckminsterfullerene[35] – as the graphene lattice cannot be bent in such a way to form a closed structure.[36] Local changes in the atomic configuration (defects) have to be introduced to create local curvature in the otherwise "flat" (although it is rolled-up) sheet and to form a hemi-spherical-like cap.[37] These defects are five-membered carbon rings, named pentagons, and their presence is believed to cause local electronic states, i.e. peaks in the local density of states (LDOS) as compared to the bulk density of states (DOS).[38] If not closed, the cap of the CNT is left open with dangling bonds, which is a less stable configuration for field emission of electrons than the closed cap configuration.[39] The position of the pentagons determines the shape of the cap, which can vary between spherical and flat.

The electrical properties of CNTs depend on the orientation of lattice parameters with respect to the tube's length; SWNTs can be either semi-conducting or metallic.[40] The electrical properties of MWNTs depend on the properties of the tubes it consists of, where a weak electronic intertube coupling exists and current is transported mostly through the outermost shells.[29,41,42]

Although the properties of CNTs change significantly depending on whether they come in bundles, other arrangements, or dispersed within a carrier medium, many consumer products are available nowadays that make use of carbon nanotubes.[43-47] Growing long CNTs to be used as fibers is one of the ultimate goals, [48] yet another approach to make material primarily based upon CNTs is to spin yarns out of samples containing many CNTs.[49,50] Some examples of single CNT applications are the single-electron CNT field effect transistor,[51] an ultrasensitive CNT mass sensor,[52] a CNT radio transmitter/receiver,[53] and scanning probe microscopy tips.[54-56]

1.4 Carbon nanotube and other novel electron sources

Due to the unique properties of carbon nanotubes – see the previous section – they have already been used to study field emission, as described in the PhD thesis by Fransen.[57] Their strength and size make them candidates for stable (cold) field emission sources with a low energy spread and high brightness. The characterization and understanding of field emission from carbon nanotubes and any other nano-materials is needed, to make best use of their properties for next generation electron sources.

1.4.1 Carbon nanotube electron sources

Using a carbon nanotube, a source from a very strong material can be constructed that permits high current densities, has a small (emitting) area at its end where several sites with a high density of states exist.[58] Besides this, CNTs can be heated up to high temperatures, which is beneficial for the removal of adsorbed species, and have a high aspect ratio due to which a relatively low potential difference between anode and cathode already causes the electric field strength to exceed the

typically needed value for field emission, ~10^9 V/m.

As field emission will most likely occur at positions where the electric field strength is highest, for a CNT this means emission is most likely to occur at its apex. The existence of a fullerene-like cap is believed to determine the emission stability. Without such a fullerene-like cap, a so-called open cap, the emission current shows instabilities, probably due to the existence of dangling bonds.[59] FEM patterns of such open CNTs show temporal and spatial fluctuations within the beam.[39] As was shown by de Jonge et al., it is possible to create a closed cap again after having cut a CNT to a specific length first. Such a closed cap structure shows improved stability that is visible both in the current and in the FEM pattern. However, it did not show the beam profile as obtained from pristine as-grown closed capped MWNTs, with several localized regions of high emission current density.[60] These regions are attributed to regions of high local density of states,[38,58] but their exact relation to field emission is not yet clear. In between such local regions of high emission current density, fringe-like features are found that are attributed to electron interference.

1.4.2 Nanowire electron sources

Besides CNTs, other materials exist with interesting properties for field emission. Nanowires with a 1D density of states can be of interest, as their energy levels are occupied in a completely different way then a 3D quantum system.[61] Systems with such a density of states might be used to obtain an electron beam with a very low energy spread. However, the effects of band bending on the DOS of such systems under application of a large electric field are not yet known. Will there be enough free charge carriers? Another question is whether or not such structures will survive field emission. Do they meet the necessary requirements regarding stability, lifetime and brightness? Following research and theoretical calculations performed by Antonio Calvosa, Lou-Fé Feiner, Erik Bakkers and Niels de Jonge, measurements on indium-arsenide (InAs) nanowires are presented in Chapter 7 of this thesis. These nanowires were characterized before and after measurements using TEM and EDX.

1.5 Research questions

In the previous section on novel field emission sources, already a few points were mentioned that need clarification. Regarding field emission from carbon nanotubes several questions can be asked.

What do we see when we image the field emission pattern of a closed or open CNT? As the cap, open or closed, is at the very end of the CNT, this will be the position at which the applied electric field strength will be highest and most electrons are expected to leave the CNT. Hence, a FEM pattern will be a magnified map of the CNT end showing the locations with highest emission probability, which is affected by the local electric field strength, work function, and density of states. As can be concluded from experiments performed by other groups, the state of the cap of a carbon nanotube affects its emission properties significantly.[62-64] Additionally, it is necessary to consider the electron trajectories from a particular position on the cap to the screen.

Having a fullerene-like capped CNT emitter, it is argued that emission comes from the carbon atoms within the pentagon rings and that therefore a very small (virtual) source size is to be expected. The diameter of a pentagonal carbon ring equals 0.248 nm.[65] However, as has been calculated theoretically, the area with a high LDOS might be larger than the pentagon area.[66] We believe it is possible to use field emission microscopy on closed CNTs to reveal the emission sites and to determine their sizes. To do so, the geometry of the emitting structure and the magnification of the FEM should be known in order to calculate the corresponding sizes on the CNT cap from the FEM pattern. The information about the size and structure of the CNT needed to do this can be obtained by imaging the source in a TEM after the field emission measurements.

If the shape of the CNT cap is purely hemispherical, a configuration that is achieved with a central pentagon and five surrounding pentagons at equal distances from the center, the electric field strength can be assumed to be constant over the entire cap. Assuming the work function does not vary significantly over the cap, the FEM pattern will then show the LDOS. By comparing FEM images on small and

large diameter CNTs, only large diameter CNTs have clearly shown six localized emission sites at the CNT cap,[60] whereas small diameter CNTs show different emission patterns.[67] So to study the properties of local emission sites of carbon nanotubes, we have used relatively large ~10 nm diameter MWNTs.

Due to the transverse energy spread of the electrons – the normal energy determines its tunneling probability – the LDOS information in the FEM pattern is blurred. By calculating the field emission energy distribution (FEED), it is possible to estimate the tunneling parameter and to simulate the transverse energy beam broadening by means of a point spread function (PSF). This PSF can then be used for deconvolution of the FEM pattern and should reveal in more detail the LDOS at the CNT cap.

By mounting a single emitting MWNT without destroying its as-grown cap, we also believe it is possible to determine the origin of interference fringes observed in FEM patterns. These interference fringes are assumed to be single-nanotube effects, however, those measurements were performed using a sample containing many emitting CNTs.[68] To make sure this interference is not a multiple-CNT effect, we have constructed a source with only one emitting CNT.

On the mechanism behind the formation of interference fringes two different theories exist. One claims the interference pattern is built up from electrons interfering with the Fermi-wavelength, hence the FEM pattern shows a magnification of the electron wavefunction at the CNT cap; the phase difference between two paths from different emission sites towards a point on the screen of the FEM is believed to be zero and not to depend on the acceleration voltage.[69] Alternatively, the electrons may interfere with the wavelength obtained during their acceleration.[68] By measuring the interference fringe spacing as function of the extraction/acceleration voltage on a single emitting CNT, as presented at the end of Chapter 6, we have ruled out the possibility that the interference is already present on the cap.

Following up on the cap closing experiments on thin MWNTs (having approximately 5 walls) by de Jonge et al., we think it should be possible to create a closed cap showing localized emission sites using a MWNT that has been cut to length after

mounting it onto a support tip, i.e. having removed its as-grown cap. Possibly the experiments by de Jonge did not show similar FEM patterns as the ones by Saito,[60] either due to their small diameter or due to a more amorphous carbon cap. We have used large (~10 nm) diameter MWNTs, and combined heat treatment and field emission experiments to induce a reorganization of the carbon atoms in the CNT apex. In Chapter 5 we will address the questions if it is possible to close such a cap, to enhance its graphitization and to change the shape of such a cap and what FE properties the resulting structure will show.

1.6 Results and discussion, summary, and future outlook

In Chapter 6 of this thesis we describe the measurements that provide a better understanding of local emission sites and interference effects visible in electron emission patterns from CNTs. First of all, such emission sites are measured to be larger than the diameter of a single pentagon. Also the virtual source size measurement shows a larger value. We demonstrated the interference is a single nanotube effect, and it appears that the interference pattern obtained is not a magnification of the electron wavefunction at the cap, but it is caused by phase differences between paths from different emission sites at the CNT cap towards the measurement screen, and is related to the extraction voltage and hence to the De Broglie wavelength of the electrons. (A simple analytical model yielded similar results as those which were obtained from measurements.) These results were obtained from unmodified, as-grown nanotubes.

Similar local emission sites were also reproduced using modified CNTs, i.e. MWNTs that were cut to length during the source mounting procedure inside the SEM. In the process of field emission and heating, changes in the cap structure were induced, which were also visible in the FEM pattern and the emission stability. If this process is further improved upon, it should be possible to obtain robust MWNT emitters with specified sizes and well graphitized caps that exhibit stable emission, low energy spread and a high brightness. The typical pattern of a well graphitized MWNT can be used to check the source status if, for example, used in a TEM.

To select and mount such CNT field emitters, a compact multi-purpose nanomanipulator for use inside the electron microscope was constructed, that is described in Chapter 3. This was followed by a patent application and hopefully the commercialization into a commercial product,[70] as the techniques developed and used for electron source fabrication proved to be useful for other applications as well, like high aspect-ratio probes for AFM studies on rough surfaces, electrochemical probes and manipulation of single spin nano-objects to build quantum bit circuits.[71]

To end this short summary of obtained results, single, closed CNT field emitters are being used now to study the fundamental limit on brightness imposed by the Pauli exclusion principle.[72] The goal of this research, performed at Vanderbilt University, is to obtain a quantum degenerate electron beam, where the entire phase space is filled with electrons.

1.7 Layout of this thesis

This thesis contains the following chapters:

Chapter 1	Introduction
Chapter 2	Theory of electron field emission and of the field emission microscope – the instrument used to record electron beam profiles
Chapter 3	Nanomanipulator – design, construction, specifications and applications of the device to produce microscopy probes within the SEM
Chapter 4	Mounting Techniques – how we enhance our probes using nano-objects
Chapter 5	Closing Experiments – experiments to close a cut MWNT and to re-graphitize its cap to obtain emission from local emission sites
Chapter 6	Closed MWNTs – experiments on unmodified, closed capped MWNTs
Chapter 7	Nanowires – characterization of the field emission properties of these structures and analysis of their structure and morphology

afterwards using TEM and EDX

References

1. R. F. Egerton *Physical Principles of Electron Microscopy: An Introduction to TEM, SEM, and AEM*. Springer, (2005).

2. D. J. Griffiths *Introduction to Electrodynamics*. Prentice-Hall, New Jersey (1999).

3. H. H. Rose. Optics of high-performance electron microscopes. *Science and Technology of Advanced Materials* **9**, 014107 (2008).

4. P. D. Nellist, M. F. Chisholm, N. Dellby, O. L. Krivanek, M. F. Murfitt, Z. S. Szilagyi, A. R. Lupini, A. Borisevich, W. H. Sides Jr. and S. J. Pennycook. Direct Sub-Angstrom Imaging of a Crystal Lattice. *Science* **305**, 1741 (2004).

5. Richard Young, Todd Templeton, Laurent Roussel, Ingo Gestmann, Gerard van Veen, Trevor Dingle and Sander Henstra. Extreme High-Resolution SEM: A Paradigm Shift. *Microscopy Today* **16**, 24-28 (2010).

6. FEI website, *http://www.fei.com/products/sem/nova-nanosem/*

7. Hitachi website, *http://hitachi-hta.com/products/electron-microscopes-and-focused-ion-beam/field-emission-sem/su9000-uhr-fe-sem*

8. R. Erni, M. D. Rossell, C. Kisielowski and U. Dahmen. Atomic-Resolution Imaging with a Sub-50-pm Electron Probe. *Physical Review Letters* **102**, 096101 (2009).

9. H. Müllejans and J.Bruley. Electron energy-loss spectroscopy (EELS) ; comparison with X-ray analysis. *J. Phys. IV France* **03**, C7-2083 (1993).

10. R. F. Egerton. Electron energy-loss spectroscopy in the TEM. *Reports on*

Progress in Physics **72**, 016502 (2009).

11. D. R. S. Cumming, S. Thoms, S. P. Beaumont and J. M. R. Weaver. Fabrication of 3 nm wires using 100 keV electron beam lithography and poly(methyl methacrylate) resist. *Applied Physics Letters* **68**, 322-324 (1996).

12. E. Slot, M. J. Wieland, G. de Boer, P. Kruit, G. F. ten Berge, A. M. C. Houkes, R. Jager, T. van de Peut, J. J. M. Peijster, S. W. H. K. Steenbrink, T. F. Teepen, A. H. V. van Veen and B. J. Kampherbeek. MAPPER: high throughput maskless lithography. *Emerging Lithographic Technologies XII* **6921**, 69211P-9 (2008).

13. S. Flügge (Ed.) R. H. Good and E. W. Müller *Handbuch der Physik, XXI*. Springer Verlag, Berlin (1956).

14. A. R. Lupini and S. J. Pennycook. Localization in elastic and inelastic scattering. *Ultramicroscopy* **96**, 313-322 (2003).

15. FEI website, *http://www.fei.com/products/sem/verios-xhr/*

16. D. J. Griffiths *Introduction to Quantum Mechanics*. Prentice-Hall, New Jersey (1995).

17. P. W. Hawkes and E. Kasper *Principles of electron optics*. Academic Press, London (1989).

18. Jon Orloff (Ed.) *Handbook of Charged Particle Optics*. CRC Press, Boca Raton (1997).

19. N. de Jonge. Carbon nanotube field emitters for electron microscopes. *Philips Research Technical Note* **PR-TN2001/251** (2001).

20. L. W. Swanson and G. A. Schwind. A Review of the Zr/O Schottky Cathode *in Handbook of charged particle optics*. J. Orloff (ed.), CRC Press, New York, 77-102 (1997).

21. M. Doytcheva, M. Kaiser and N. de Jonge. In situ transmission electron microscopy investigation of the structural changes in carbon nanotubes during electron emission at high currents. *Nanotechnology* **17**, 3226-3233 (2006).

22. S. Iijima. Helical microtubules of graphitic carbon. *Nature* **354**, 56-58 (1991).

23. M. Monthioux and V. L. Kuznetsov. Who should be given the credit for the discovery of carbon nanotubes? *Carbon* **44**, 1621-1623 (2006).

24. S. Iijima and T. Ichihashi. Single-shell carbon nanotubes of 1-nm diameter. *Nature* **363**, 603-605 (1993).

25. D. S. Bethune, C. H. Klang, M. S. de Vries, G. Gorman, R. Savoy, J. Vazquez and R. Beyers. Cobalt-catalysed growth of carbon nanotubes with single-atomic-layer walls. *Nature* **363**, 605-607 (1993).

26. B. Q. Wei, R. Vajtai and P. M. Ajayan. Reliability and current carrying capacity of carbon nanotubes. *Applied Physics Letters* **79**, 1172-1174 (2001).

27. Z. Yao, C. L. Kane and C. Dekker. High-Field Electrical Transport in Single-Wall Carbon Nanotubes. *Physical Review Letters* **84**, 2941 (2000).

28. B. I. Yakobson and P. Avouris. Mechanical Properties of Carbon Nanotubes *in Carbon Nanotubes Synthesis, Structure, Properties and Applications*. M. S. Dresselhaus, G. Dresselhaus & P. Avouris (eds.), Springer-Verlag, Berlin, 287-327 (2001).

29. L. Forró and C. Schönenberger. Physical Properties of Multi-wall Nanotubes *in Carbon Nanotubes Synthesis, Structure, Properties and Applications*. M. S. Dresselhaus, G. Dresselhaus & P. Avouris (eds.), Springer-Verlag, Berlin, 329-390 (2001).

30. N. de Jonge. Carbon nanotube electron sources for electron microscopes. *Advances in Imaging & Electron Physics* **156**, 203-233 (2009).

31. M. S. Dresselhaus and M. Endo. Relation of Carbon Nanotubes to Other Carbon Materials *in Carbon Nanotubes Synthesis, Structure, Properties and Applications*. M. S. Dresselhaus, G. Dresselhaus & P. Avouris (eds.), Springer-Verlag, Berlin, 11-28 (2001).

32. P. M. Ajayan and O. Zhou. Applications of Carbon Nanotubes *in Carbon Nanotubes Synthesis, Structure, Properties and Applications*. M. S. Dresselhaus, G. Dresselhaus & P. Avouris (eds.), Springer-Verlag, Berlin, 391-425 (2001).

33. A. Kis, G. Csanyi, J. P. Salvetat, T. N. Lee, E. Couteau, A. J. Kulik, W. Benoit, J. Brugger and L. Forro. Reinforcement of single-walled carbon nanotube bundles by intertube bridging. *Nat Mater* **3**, 153-157 (2004).

34. P. M. Ajayan and F. Banhart. Nanotubes: Strong bundles. *Nat Mater* **3**, 135-136 (2004).

35. H. W. Kroto, J. R. Heath, S. C. O'Brien, R. F. Curl and R. E. Smalley. C60: Buckminsterfullerene. *Nature* **318**, 162-163 (1985).

36. R. Saito, G. Dresselhaus and M. S. Dresselhaus *Physical properties of carbon nanotubes*. Imperial College Press, London (1998).

37. S. Iijima, T. Ichihashi and Y. Ando. Pentagons, heptagons and negative curvature in graphite microtubule growth. *Nature* **356**, 776-778 (1992).

38. T. W. Odom, J.-L. Huang, P. Kim and C. M. Lieber. Structure and Electronic Properties of Carbon Nanotubes. *J. Phys. Chem. B* **104**, 2794-2809 (2000).

39. N. de Jonge, M. Doytcheva, M. Allioux, M. Kaiser, S. A. M. Mentink, K. B. K. Teo, R. G. Lacerda and W. I. Milne. Cap Closing of Thin Carbon Nanotubes. *Adv. Mater.* **17**, 451-455 (2005).

40. S. G. Louie. Electronic Properties, Junctions, and Defects of Carbon Nanotubes *in Carbon Nanotubes Synthesis, Structure, Properties and Applications*. M. S. Dresselhaus, G. Dresselhaus & P. Avouris (eds.), Springer-Verlag, Berlin, 113-145 (2001).

41. B. Bourlon, C. Miko, L. Forró, D. C. Glattli and A. Bachtold. Determination of the Intershell Conductance in Multiwalled Carbon Nanotubes. *Physical Review Letters* **93**, 176806 (2004).

42. J. C. Charlier, X. Blase and S. Roche. Electronic and transport properties of nanotubes. *Rev. Mod. Phys.* **79**, 677 (2007).

43. La Sportiva ski's, *http://www.sportiva.com/resources/images/Product_Images/TechSheets/VaporNano_techsheet.pdf*

44. Review on BMC bicycle using Easton CNT technology, *http://www.pezcyclingnews.com/page/tech-n-spec/?id=88739*

45. Easton CNT bat commercial, *http://www.youtube.com/watch?v=ORWyDSluw8g*

46. L. Xiao, Z. Chen, C. Feng, L. Liu, Z. Q. Bai, Y. Wang, L. Qian, Y. Zhang, Q. Li, K. Jiang and S. Fan. Flexible, Stretchable, Transparent Carbon Nanotube Thin Film Loudspeakers. *Nano Lett.* **8**, 4539-4545 (2008).

47. Zyvex sports case studies, *http://www.zyvextech.com/sports*

48. Q. Wen, W. Qian, J. Nie, A. Cao, G. Ning, Y. Wang, L. Hu, Q. Zhang, J. Huang and F. Wei. 100 mm Long, Semiconducting Triple-Walled Carbon Nanotubes. *Adv. Mater.* **22**, 1867-1871 (2010).

49. M. Zhang, K. R. Atkinson and R. H. Baughman. Multifunctional Carbon Nanotube Yarns by Downsizing an Ancient Technology. *Science* **306**, 1358-1361 (2004).

50. K. Jiang, Q. Li and S. Fan. Nanotechnology: Spinning continuous carbon nanotube yarns. *Nature* **419**, 801 (2002).

51. H. W. C. Postma, T. Teepen, Z. Yao, M. Grifoni and C. Dekker. Carbon Nanotube Single-Electron Transistors at Room Temperature. *Science* **293**, 76-79 (2001).

52. B. Lassagne, D. Garcia-Sanchez, A. Aguasca and A. Bachtold. Ultrasensitive Mass Sensing with a Nanotube Electromechanical Resonator. *Nano Lett.* **8**, 3735-3738 (2008).

53. K. Jensen, J. Weldon, H. Garcia and A. Zettl. Nanotube Radio. *Nano Lett.* **7**, 3508-3511 (2007).

54. M. H. van Es. A new touch to atomic force microscopy: smart probing of biological and biomedical systems at the nanoscale. Ph.D. thesis, Leiden University (2008).

55. A. J. Katan and T. H. Oosterkamp. Measuring Hydrophobic Interactions with Three-Dimensional Nanometer Resolution. *J. Phys. Chem. C* **112**, 9769-9776 (2008).

56. A. V. Patil, A. F. Beker, F. G. M. Wiertz, H. A. Heering, G. C. Coslovich,

R. Vlijm and T. H. Oosterkamp. Fabrication and characterization of polymer insulated carbon nanotube modified electrochemical nanoprobes. *Nanoscale* **2**, 734-738 (2009).

57. M. J. Fransen. Towards high-brightness, monochromatic electron sources. Delft University of Technology (1998).

58. P. Kim, T. W. Odom, J.-L. Huang and C. Lieber. Electronic Density of States of Atomically Resolved Single-Walled Carbon Nanotubes: Van Hove Singularities and End States. *Phys. Rev. Lett.* **82**, 1225-1228 (1999).

59. A. G. Rinzler, J. H. Hafner, P. Nikolaev, P. Nordlander, D. T. Colbert, R. E. Smalley, L. Lou, S. G. Kim and D. Tomanek. Unraveling Nanotubes: Field Emission from an Atomic Wire. *Science* **269**, 1550-1553 (1995).

60. Y. Saito, K. Hata and T. Murata. Field Emission Patterns Originating from Pentagons at the Tip of a Carbon Nanotube. *Jpn. J. Appl. Phys.* **39**, L271-L272 (2000).

61. Charles Kittel *Introduction to Solid State Physics*. John Wiley & Sons, New York (1996).

62. N. de Jonge, M. Allioux, M. Doytcheva, M. Kaiser, K. B. K. Teo, R. G. Lacerda and W. I. Milne. Characterization of the field emission properties of individual thin carbon nanotubes. *Appl. Phys. Lett.* **85**, 1607-1609 (2004).

63. K. A. Dean and B. R. Chalamala. Field emission microscopy of carbon nanotube caps. *Journal of Applied Physics* **85**, 3832-3836 (1999).

64. K. A. Dean and B. R. Chalamala. Experimental studies of the cap structure of single-walled carbon nanotubes. *J. Vac. Sci. Technol. B* **21**, 868-871 (2003).

65. K. Hedberg, L. Hedberg, D. S. Bethune, C. A. Brown, H. C. Dorn, R. D. Johnson and M. De Vries. Bond Lengths in Free Molecules of Buckminsterfullerene, C60, from Gas-Phase Electron Diffraction. *Science* **254**, 410-412 (1991).

66. A. De Vita, J. C. Charlier, X. Blase and R. Car. Electronic structure at carbon nanotube tips. *Appl. Phys. A: Mater. Sci. Process.* **68**, 283-286 (1999).

67. M. Khazaei, K. A. Dean, A. A. Farajian and Y. Kawazoe. Field Emission Signature of Pentagons at Carbon Nanotube Caps. *J. Phys. Chem. C* **111**, 6690-6693 (2007).

68. K. Hata, A. Takakura, K. Miura, A. Ohshita and Y. Saito. Interference fringes observed in electron emission patterns of a multiwalled carbon nanotube. *J. Vac. Sci. Technol. B* **22**, 1312-1314 (2004).

69. C. Oshima, K. Mastuda, T. Kona, Y. Mogami, M. Komaki, Y. Murata, T. Yamashita, T. Kuzumaki and Y. Horiike. Young's Interference of Electrons in Field Emission Patterns. *Phys. Rev. Lett.* **88**, 038301 (2002).

70. D. J. van der Zalm, E. C. Heeres, M. B. S. Hesselberth, A. J. Katan, and M. H. van Es. A nano-scale manipulator. U.K.Patent Application GB0908780.0 (2010)

71. T. van der Sar, E. C. Heeres, G. M. Dmochowski, G. de Lange, L. Robledo, T. H. Oosterkamp and R. Hanson. Nanopositioning of a diamond nanocrystal containing a single nitrogen-vacancy defect center. *Appl. Phys. Lett.* **94**, 173104-3 (2009).

72. J. D. Jarvis, H. L. Andrews, B. Ivanov, C. L. Stewart, N. de Jonge, E. C. Heeres, W. P. Kang, Y. M. Wong, J. L. Davidson and C. A. Brau. Resonant tunneling and extreme brightness from diamond field emitters

and carbon nanotubes. *J. Appl. Phys.* **108**, 094322-094326 (2010).